The Abelson tyrosine kinase, the Trio GEF and Enabled interact with the Netrin receptor Frazzled in *Drosophila*

David J. Forsthoefel[1], Eric C. Liebl[2], Peter A. Kolodziej[3,*] and Mark A. Seeger[1,†]

[1]The Ohio State University, Department of Molecular Genetics and Center for Molecular Neurobiology, Columbus, OH 43210, USA
[2]Denison University, Department of Biology, Granville, OH 43023, USA
[3]Vanderbilt University Medical Center, Department of Cell and Developmental Biology, Center for Molecular Neuroscience, MCN C2210, Nashville, TN 37232-2175, USA

*We celebrate the life of our friend and colleague Peter Kolodziej who passed away 3 March 2005. Peter was an inquisitive and insightful scientist who will be missed.
†Author for correspondence (e-mail: seeger.9@osu.edu)

Accepted 2 February 2005

Development 132, 1983-1994
Published by The Company of Biologists 2005
doi:10.1242/dev.01736

Summary

The attractive Netrin receptor Frazzled (Fra), and the signaling molecules Abelson tyrosine kinase (Abl), the guanine nucleotide-exchange factor Trio, and the Abl substrate Enabled (Ena), all regulate axon pathfinding at the *Drosophila* embryonic CNS midline. We detect genetic and/or physical interactions between Fra and these effector molecules that suggest that they act in concert to guide axons across the midline. Mutations in *Abl* and *trio* dominantly enhance *fra* and *Netrin* mutant CNS phenotypes, and *fra;Abl* and *fra;trio* double mutants display a dramatic loss of axons in a majority of commissures. Conversely, heterozygosity for *ena* reduces the severity of the CNS phenotype in *fra*, *Netrin* and *trio,Abl* mutants. Consistent with an in vivo role for these molecules as effectors of Fra signaling, heterozygosity for *Abl*, *trio* or *ena* reduces the number of axons that inappropriately cross the midline in embryos expressing the chimeric Robo-Fra receptor. Fra interacts physically with Abl and Trio in GST-pulldown assays and in co-immunoprecipitation experiments. In addition, tyrosine phosphorylation of Trio and Fra is elevated in S2 cells when Abl levels are increased. Together, these data suggest that Abl, Trio, Ena and Fra are integrated into a complex signaling network that regulates axon guidance at the CNS midline.

Key words: *Drosophila*, CNS midline, Axon guidance, Abelson tyrosine kinase, Abl, Trio, Guanine nucleotide-exchange factor, Enabled, Frazzled, Netrin, Actin cytoskeleton, Growth cone attraction

Introduction

Extracellular guidance cues, their receptors on the growth cone surface, and intracellular effectors function together to regulate directional axon extension (Dent and Gertler, 2003; Guan and Rao, 2003; Huber et al., 2003; Lee and Van Vactor, 2003; Luo, 2002). Genetic screens for mutants defective in axon pathfinding at the midline in the *Drosophila* embryo have identified many of these evolutionarily conserved molecules, and suggest that growth cones respond to a balance of extracellular matrix chemoattractants (e.g. Netrins) and chemorepellents (e.g. Slit) (Araujo and Tear, 2003). *frazzled* (*fra*) encodes an attractive Netrin receptor related to mammalian Deleted in Colorectal Cancer (DCC) and *C. elegans* UNC-40 (Chan et al., 1996; Keino-Masu et al., 1996; Kolodziej et al., 1996). Mutations that remove both of the closely related *Netrin* genes, or mutations in *fra*, result in thin or missing commissural axon bundles, reflecting a decrease in growth cone attraction to the central nervous system (CNS) midline (Harris et al., 1996; Kolodziej et al., 1996; Mitchell et al., 1996). Conversely, members of the Roundabout (Robo) family of Slit receptors mediate repulsion, and mutations in *slit* or in *robo* receptors cause CNS growth cones to cross the midline inappropriately (Battye et al., 1999; Kidd et al., 1999; Kidd et al., 1998; Rajagopalan et al., 2000; Rothberg et al., 1988; Seeger et al., 1993; Simpson et al., 2000a; Simpson et al., 2000b).

An emerging theme in axon guidance is that growth cone receptors recruit cytoplasmic effectors to modulate reorganization of the actin cytoskeleton (Huber et al., 2003; Patel and Van Vactor, 2002). Relatively little is known about how Frazzled and its homologs DCC and UNC-40 signal to the cytoskeleton during axon guidance and outgrowth. A screen in *C. elegans* for genetic suppressors of an UNC-40 gain-of-function phenotype identified molecules that may function with UNC-40 and Netrin/UNC-6 to regulate actin dynamics (Gitai et al., 2003). These include the actin-binding protein AbLIM/UNC-115, Enabled (Ena)/UNC-34, and the Rho-family guanosine triphosphatase (GTPase) Rac/CED-10. AbLIM/UNC-115 behaves genetically as an effector of signaling by the Rac-2 GTPase (Struckhoff and Lundquist, 2003). The vertebrate orthologs of Ena/UNC-34, Mena, vasodilator-stimulated protein (VASP) and Ena/VASP-like (EVL), antagonize F-actin capping and allow F-actin filament elongation (Bear et al., 2002; Gitai et al., 2003). Netrin stimulation of cultured mouse neurons results in Ena/VASP-dependent filopodia formation and Mena phosphorylation at a protein kinase A regulatory site (Lebrand et al., 2004). In cultured vertebrate cells, the adaptor Nck1 and the GTPases

Cdc42 and Rac1 affect Netrin- and DCC-dependent neurite outgrowth, cell spreading and filopodia extension (Li et al., 2002a; Li et al., 2002b; Shekarabi and Kennedy, 2002). Nck1 binds DCC in vitro, and can regulate actin nucleation in concert with Rac through WAVE1, an Arp2/3 complex activator; however, it is not known whether the WAVE complex is activated in response to Netrin-DCC signaling (Eden et al., 2002; Li et al., 2002a). Similarly, although Netrin stimulation of DCC-expressing non-neuronal cells leads to activation of Cdc42 and Rac1, the mechanisms by which DCC regulates small GTPase activity have not been elucidated (Li et al., 2002b; Shekarabi and Kennedy, 2002).

Other pathways from DCC to the F-actin cytoskeleton are likely to involve cytoplasmic tyrosine kinases. DCC interacts with focal adhesion kinase (FAK), Src and Fyn, and DCC is tyrosine phosphorylated in cells expressing increased levels of these kinases or upon Netrin stimulation; furthermore, phosphorylation of DCC is required for attractive axon turning in cultured neurons and Rac1 activation in non-neuronal cells (Li et al., 2004; Liu et al., 2004; Meriane et al., 2004; Ren et al., 2004). Tyrosine phosphorylation of UNC-40 has also been observed, and genetic interactions indicate that UNC-40 signaling is regulated by the receptor protein tyrosine phosphatase (RPTP) CLR-1 (Chang et al., 2004; Tong et al., 2001).

In *Drosophila*, signaling by Fra and the Netrins is even less understood. Genetic interactions with *fra* suggest that *Gef64C*, *weniger*, *Arf6-Gef/Schizo*, *Myosin Light Chain Kinase* (*Stretchin-Mlck* – FlyBase) and the G-protein *Gαq* (*Gαq49B* – FlyBase) promote commissure formation (Bashaw et al., 2001; Hummel et al., 1999a; Hummel et al., 1999b; Kim et al., 2002; Onel et al., 2004; Ratnaparkhi et al., 2002). However, none of the molecules encoded by these genes nor any others have been linked biochemically to Fra signaling.

The *Drosophila* Abelson cytoplasmic tyrosine kinase (Abl), the Trio Rac/Rho guanosine-exchange factor (GEF) and Ena are expressed in the nervous system and interact genetically and/or biochemically with receptors known to regulate nervous system development (Awasaki et al., 2000; Bashaw et al., 2000; Bateman et al., 2000; Crowner et al., 2003; Gertler et al., 1989; Gertler et al., 1995; Liebl et al., 2003; Wills et al., 1999). These molecules and their homologs in other organisms regulate cytoskeletal dynamics during diverse developmental processes (Bateman and Van Vactor, 2001; Hakeda-Suzuki et al., 2002; Kwiatkowski et al., 2003; Lanier and Gertler, 2000; Moresco and Koleske, 2003; Van Etten, 1999; Woodring et al., 2003). In cultured cells, these molecules regulate cell migration, neurite extension and leading edge actin dynamics (Bateman and Van Vactor, 2001; Estrach et al., 2002; Kwiatkowski et al., 2003; Moresco and Koleske, 2003).

In this study, we expand the understanding of the signaling networks in which Abl, Trio and Ena function by uncovering genetic and biochemical interactions between these molecules and the Netrin receptor Fra. Our results indicate that Abl, Trio and Ena probably function as effectors of Fra signaling in commissural axons, in addition to roles downstream of other growth cone receptors. Furthermore, our observations suggest potential mechanisms by which Fra and other receptors might coordinate actin cytoskeletal dynamics through these molecules.

Materials and methods

Genetics and immunohistochemistry

The following alleles/chromosomes were used: *fra*^{4}; *Df(2R)vg135,nompA*^{vg135} (*Df(2R)vg135* is a chromosomal deficiency that removes *fra*); *Df(1)NP5* (removes *NetA* and *NetB*); *ena*^{GC10}; *ena*^{GC5}; *ena*^{210}; *ena*^{23}; *Abl*^{1}; *Abl*^{4}; *Df(3L)st-j7* (removes *Abl*); *trio*^{M89}; *Df(3L)FpaI* (removes *trio*); *trio*$^{P0368/10}$; *trio*$^{IMP159.4}$ (an imprecise excision allele generated by mobilizing the P-element in *trio*$^{P0368/10}$); *trio*^{M89},*Abl*^{1}; *Df(3L)FpaI,Abl*^{4}; *trio*$^{IMPT59.4}$,*Abl*^{1}; and UAS-Robo-Fra-Myc (kindly provided by Greg Bashaw). *fra*^{4},*ena*^{GC10} recombinant chromosomes were generated by meiotic recombination and isolated on the basis of their failure to complement both *ena*^{GC8} and *Df(2R)vg135*.

All flies were maintained in standard cornmeal-yeast medium at room temperature. Embryos were fixed in 4% paraformaldehyde/1×PBS, and the CNS was visualized using mAb BP102 (1:20, Developmental Studies Hybridoma Bank, University of Iowa), anti-β-galactosidase (1:500, Promega), goat anti-mouse-HRP (1:500, Jackson), and standard immunohistochemical procedures (Patel et al., 1987). All alleles were maintained over *lacZ*-expressing balancers to distinguish the genotype of embryos. Stage 14-16 embryos were filleted and scored at 400× magnification.

Constructs

pMET Abl-Myc, pMET Trio-Myc, pMET Trio$^{\Delta SPR}$-Myc, pMET Fra-Myc, pMET Fra-HA, pMET Fra$^{\Delta CYTO}$-HA [deleted for amino acids P1123-C1375 (GenBank Accession Number U71001)], pBSK Abl-Myc, pBKS Trio-Myc, pBKS Trio$^{\Delta SPR}$-Myc [deleted for amino acids L285-D1199 (GenBank Accession Number AF216663)], pBSK Ena-Myc, pGEX2T-Fra$_{CYTO}$ [amino acids C1098-C1375 (GenBank Accession Number U71001)], pGEX2T-AblSH3 [amino acids E202-K268 (GenBank Accession Number AH001049)], and pGEX2T-TrioSH3 [amino acids E1177-L1840, deleted for GEF1 (A1281-P1596) (GenBank Accession Number AF216663)] were all constructed using standard molecular techniques; details are available upon request. pPAC Ena was provided by A. Comer (Comer et al., 1998). pMET Fra constructs were generated using the short isoform that rescues *fra* mutant phenotypes (Kolodziej et al., 1996). Myc and HA tags were added C terminally.

Protein-protein interactions and phosphorylation assays

GST and GST-Fra$_{cyto}$ were generated in *E. coli* (BL21), as described in Amersham Pharmacia's Gene Fusion System Guide. GST pulldowns of in vitro-translated proteins were performed essentially as described (Bashaw et al., 2000), except that non-radiolabeled, epitope-tagged proteins were generated in vitro using TnT T7-coupled rabbit reticulocyte lysate system (Promega), and Abl, Trio and Ena constructs cloned into pBluescript (Stratagene). An aliquot from each reaction (15-25 μl) was added to ~10 μg fusion protein bound to beads suspended in 200 μl binding buffer. Binding was overnight, and, after washing, ~20% of total protein was separated by SDS-PAGE. For GST pulldowns from S2 cell extracts, 2×10^{7} S2 cells were transiently transfected with pMET Abl-Myc, pMET Trio-Myc, or pPAC Ena with CellFectin Reagent (Invitrogen). Twenty-four hours after induction, cells were lysed in 1 ml IP buffer (Comer et al., 1998), and lysates were pre-cleared with 100 μl of Glutathione Sepharose4B beads prior to GST pulldowns.

For co-immunoprecipitations, 2×10^{7} S2 cells were transiently transfected with the relevant constructs, and 24 hours after induction, cells were rinsed once in 1×PBS then lysed in 50 mM Tris (pH 8), 100 mM NaCl, 1 mM $MgCl_2$, 1% NP-40, 10 mM NaF, 2 mM Na_3VO_4, and 5 μg/ml each of Aprotinin and Leupeptin (Roche). Cell extracts were cleared by centrifugation, lysates were pre-cleared with 40 μl Protein G Sepharose beads (Sigma) for 30 minutes, and protein complexes were immunoprecipitated with 1 μg rabbit anti-Myc (Santa Cruz), anti-Ena [5G2, Developmental Studies Hybridoma Bank

(Bashaw et al., 2000)] diluted 1:20, or anti-HA (HA.11, Covance) diluted 1:150, for 60 minutes. Immune complexes were recovered on 40 µl Protein G beads for 60 minutes, washed three to four times in lysis buffer containing 1 µg/ml Aprotinin and Leupeptin, and boiled in 6× sample buffer.

For Trio and Fra phosphorylation experiments, 2×10^7 S2 cells were transiently transfected with pMET Trio-Myc, pMET Fra-Myc, pMET Abl, and/or empty pMET vector (to control for transfection efficiency in experiments receiving less than 5 µg pMET Abl). For pervanadate treatment, cells [in Schneider's Media (BRL/Invitrogen), plus 10% FBS] were treated with 2 mM Na_3VO_4 and 3 mM H_2O_2 for 30 minutes at room temperature. In all experiments, cells were rinsed once in PBS and then lysed in 50 mM Tris (pH 8), 300 mM NaCl, 5 mM EDTA, 1% Triton X-100, 10 mM NaF, 2 mM Na_3VO_4, and 5 µg/ml each of Aprotinin and Leupeptin. After immunoprecipitation (IP), beads were washed four to six times in lysis buffer containing 1 µg/ml Aprotinin and Leupeptin, and boiled in 2× Sample Buffer.

Phosphotyrosine was detected using 4G10 mouse anti-phosphotyrosine (Upstate) at 1:10,000 and goat anti-mouse-HRP (Jackson) at 1:10,000 in low-salt TBST (25 mM NaCl)/5% BSA. Mouse anti-Myc (Roche), rabbit anti-Myc (Santa Cruz), mouse anti-HA, and rabbit anti-Abl (kindly provided by A. Comer) were used at a dilution of 1:2000 in 5% milk/TBST. Mouse anti-Ena 5G2 was used at 1:200 in 5% milk/TBST. Proteins were visualized using ECL (for phosphotyrosine detection), ECL PLUS (Amersham Pharmacia, for protein-protein interactions), or NBT/BCIP detection (for loading controls in co-IP and phosphorylation experiments). Prior to the re-probing of co-IP and phosphotyrosine westerns, blots were stripped in 50 mM Tris-HCl (pH 6.8), 2% SDS and 100 mM β-mercaptoethanol overnight at 65°C.

Results

Mutations in *Abelson* and *trio* dominantly enhance the *fra* and *Netrin* CNS phenotypes

Noting that the *trio,Abl* double mutant CNS phenotype is qualitatively similar, but much more severe, than the phenotype of *fra* mutant embryos, and that Fra, Trio and Abl localize to CNS axons, we hypothesized that these molecules collaboratively regulate commissure formation (Fig. 1A-F; Tables 1, 2, 4) (Awasaki et al., 2000; Gertler et al., 1989; Kolodziej et al., 1996; Liebl et al., 2000). Because dosage-sensitive genetic interactions often indicate that gene products function in the same biological process, we asked whether mutations in *Abl* or *trio* dominantly modify the *fra* CNS phenotype.

In homozygous *fra* (*fra*^{4}/*Df(2R)vg135*) mutant embryos, 21% of segments had defective commissures. As in a previous study (Kolodziej et al., 1996), we found that the majority of defective segments in *fra* embryos (13% in this case) had thin or missing commissures, and that the posterior commissure was most often affected (Fig. 1F, Table 1). In 8% of segments, an approximately wild-type number of axons crossed the midline, but commissures were disorganized (examples of errors are indicated in Fig. 1 and are described in the Table 1 footnotes).

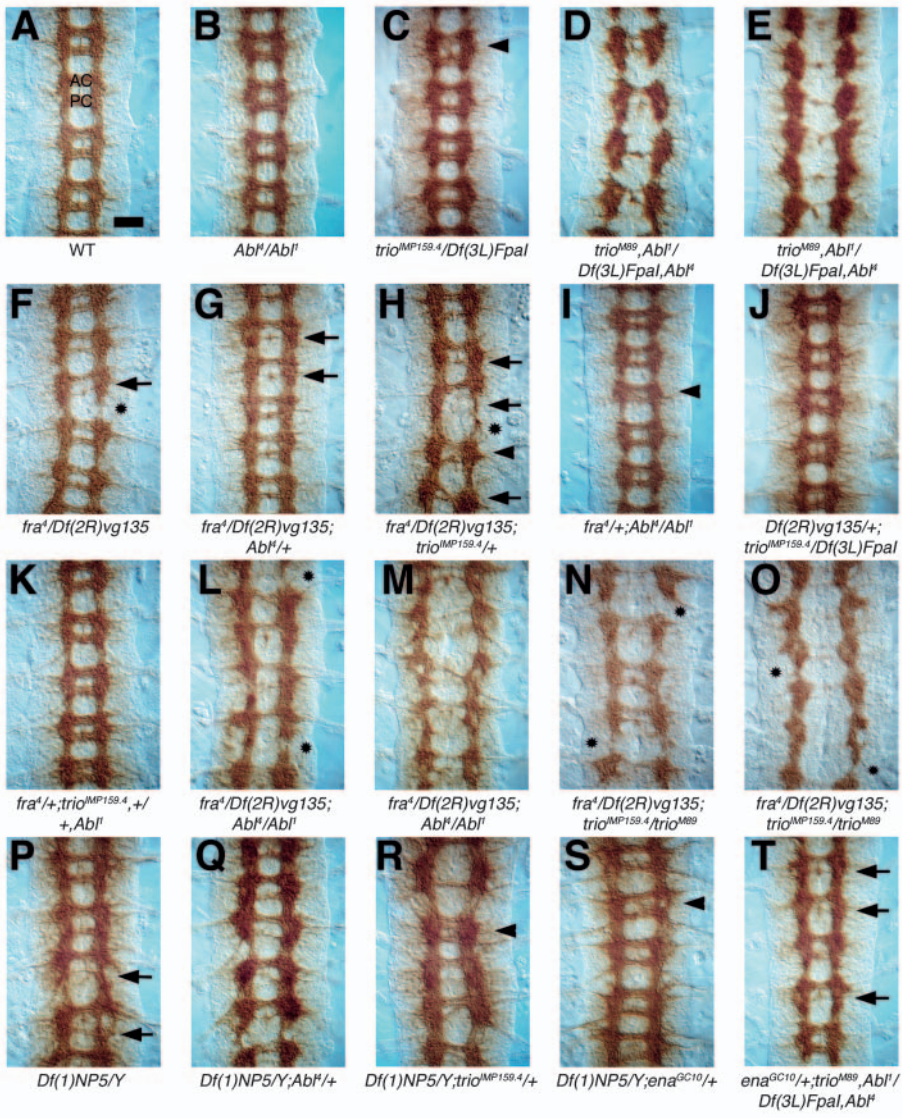

Fig. 1. *Abl*, *trio* and *ena* interact genetically with *fra* and the *Netrin* genes. CNS axons were labeled with mAb BP102, and stage 14-16 embryos were dissected and scored for defects. (A) In wild-type embryos, CNS axons are organized into two commissures per segment (AC and PC), and two longitudinal tracts that run the length of the nerve cord on either side of the midline. (B-T) In mutant embryos (genotypes are indicated in the figure), commissure formation is defective. Examples of segments with thin or missing commissures are indicated with arrows in F-H,P and T. Examples of segments with errors in commissural axon pathfinding are indicated with arrowheads in C,H,I,R and S. Examples of breaks in longitudinal pathways are indicated with asterisks in F,H,L,N and O. D,L and N are examples of moderate *trio,Abl, fra;Abl,* and *fra;trio* phenotypes, respectively, whereas E,M and O show severe phenotypes. *Df(2R)vg135* and *Df(3L)FpaI* are deficiencies for *fra* and *trio*, respectively. *Df(1)NP5* removes both *NetA* and *NetB*. Anterior is to the top of each image. Scale bar in A: ~25 µm.

Table 1. *Abl* enhances commissure defects in *fra* and *Netrin* mutant embryos

Genotype	% Defective segments, overall (*n*)	% Segments with thin/ missing commissures*	% Segments with path-finding errors†
$fra^4/Df(2R)vg135$	21 (1279)	13	8
$fra^4/Df(2R)vg135;Abl^4/+$	30 (511)	24	6
$fra^4/Df(2R)vg135;Abl^1/+$	47 (186)	39	8
$fra^4/Df(2R)vg135;Abl^4/Abl^1$	95 (166)	85	10
fra^4/fra^4	36 (212)	23	13
$fra^4/fra^4;Abl^4/+$	45 (458)	33	12
$fra^4/fra^4;Abl^1/+$	54 (215)	37	17
$fra^4/fra^4;Abl^1/Abl^4$	100 (158)	97	3
$Df(1)NP5/Y$	34 (277)	24	10
$Df(1)NP5/Y;Abl^4/+$	41 (312)	33	8
Abl^4/Abl^1	6.6 (257)	1.2	5.4
$fra^4/+;Abl^4/Abl^1$	11.8 (286)	1.0	10.8
$Df(2R)vg135/+;Abl^4/Abl^1$	19 (234)	2	17

Number of segments scored (*n*) are indicated in parentheses in column 2.

*Segments were scored as having 'thin/missing' commissures if >75% of BP102-staining axons were absent in either commissure.

†'Errors' category includes ectopic wandering or defasciculation of axons between commissures, fused commissures, and commissures that split into smaller bundles along their length, often at the junction of the commissure with the longitudinal axon tract.

Percentages were not rounded when the overall defects were less than 15%.

Table 2. *trio* enhances commissure defects in *fra* and *Netrin* mutant embryos

Genotype	% Defective segments, overall (*n*)	% Segments with thin/ missing commissures	% Segments with path-finding errors
$fra^4/Df(2R)vg135$	21 (1279)	13	8
$fra^4/Df(2R)vg135;Df(3L)FpaI/+$	33 (497)	17	16
$fra^4/Df(2R)vg135;trio^{M89}/+$	25 (185)	17	8
$fra^4/Df(2R)vg135;trio^{IMP159.4}/+$	53 (208)	42	11
$fra^4/Df(2R)vg135;trio^{IMP159.4}/trio^{M89}$	79 (172)	66	13
fra^4/fra^4	36 (212)	23	13
$fra^4/fra^4;trio^{M89}/+$	64 (262)	44	20
$fra^4/fra^4;trio^{P0368/10}/+$	69 (162)	47	22
$fra^4/fra^4;trio^{IMP159.4}/+$	90 (213)	80	10
$fra^4/fra^4;Df(3L)FpaI/+$	62 (152)	47	15
$fra^4/fra^4;trio^{IMP159.4}/trio^{M89}$	96 (118)	92	4
$fra^4/fra^4;trio^{M89}/trio^{P0368/10}$	85 (189)	75	10
$Df(1)NP5/Y$	34 (277)	24	10
$Df(1)NP5/Y;trio^{M89}/+$	43 (214)	29	14
$Df(1)NP5/Y;trio^{IMP159.4}/+$	71 (143)	56	15
$trio^{IMP159.4}/Df(3L)FpaI$	6.4 (421)	1.9	4.5
$fra^4/+;trio^{IMP159.4}/Df(3L)FpaI$	3.3 (216)	0.5	2.8
$Df(2R)vg135/+;trio^{IMP159.4}/Df(3L)FpaI$	6.1 (195)	1.0	5.1
$trio^{IMP159.4}/trio^{M89}$	9.9 (354)	4.8	5.1
$fra^4/+;trio^{IMP159.4}/trio^{M89}$	5.9 (153)	1.3	4.6

Percentages were not rounded when overall defects were less than 15%.

In homozygous *fra*, heterozygous *Abl* ($fra^4/Df(2R)vg135;Abl^4/+$) embryos, the percentage of segments with defective commissures increased to 30%, and this increase was due solely to an increase in the number of thin or missing commissures (24%, Fig. 1G, Table 1). The independently generated Abl^1 allele also dominantly enhanced the *fra* phenotype, demonstrating that lesions in *Abl* were responsible for the genetic interaction with *fra*, and not accessory mutations on any of the chromosomes tested (Table 1).

Heterozygosity for *trio* also enhanced the CNS phenotype in *fra* mutant embryos. For example, in $fra^4/Df(2R)vg135;trio^{IMP159.4}/+$ embryos, 53% of segments had defective commissures (Fig. 1H, Table 2). Forty-two percent of segments in $fra^4/Df(2R)vg135;trio^{IMP159.4}/+$ embryos had thin or missing commissures (versus 13% in $fra^4/Df(2R)vg135$ animals), and 11% of segments had commissural pathfinding errors (versus 8% in $fra^4/Df(2R)vg135$ embryos) (Fig. 1H, Table 2). Milder dominant enhancement of the *fra* phenotype was observed for a number of other *trio* alleles, including the deficiency *Df(3L)FpaI*, the hypomorphic P-element insertion allele $trio^{P0368/10}$, and the $trio^{M89}$ allele (which encodes a point mutation in the GEF1 domain of Trio) originally identified as a dominant enhancer of the *Abl* semilethality phenotype (Liebl et al., 2000) (Table 2). It is not clear why $trio^{IMP159.4}$ (an imprecise excision allele generated by mobilizing the P element on the $trio^{P0368/10}$ chromosome) enhances the *fra* phenotype so strongly. As the deficiency *Df(3L)FpaI* (which completely removes the *trio* gene) behaves similarly to the other *trio* alleles we tested, it is likely that $trio^{IMP159.4}$ is not a null or hypomorphic allele, but rather encodes a Trio protein with unusual properties. It is also not clear why fra^4 homozygotes have more disrupted commissures than $fra^4/Df(2R)vg135$ animals (this *fra* allele has not been characterized), although fra^4 homozygous animals are not immunoreactive with the polyclonal anti-*fra* serum generated by Kolodziej et al. (Kolodziej et al., 1996).

Although in most *fra* mutant combinations tested the posterior commissure (PC) was affected more often than the anterior commissure (AC), heterozygosity for *Abl* or *trio* increased the frequency of defects in both commissures. For example, in fra^4/fra^4 embryos 20% (*n*=212) of PCs scored were thin or missing, versus 31% (*n*=215) in $fra^4/fra^4;Abl^1/+$ mutants and 39% (*n*=262) in $fra^4/fra^4;trio^{M89}/+$ embryos. Similarly, 5% (*n*=212) of ACs scored were thin or missing in fra^4/fra^4 embryos, versus 14% (*n*=215) in the $fra^4/fra^4;Abl^1/+$ background and 18% (*n*=262) in $fra^4/fra^4;trio^{M89}/+$ embryos. Thus, although mutations in *fra* seem to affect posterior commissural axons preferentially (Kolodziej et al., 1996), the genetic interactions of *fra* with *Abl* and *trio* are consistent with a significant role for all of these genes in anterior commissure formation as well.

We next asked whether heterozygosity for *Abl* or *trio* modifies the CNS phenotype in embryos mutant for genes encoding the Frazzled ligands *Netrin A and Netrin B*. *NetA* and *NetB* are both removed by a deficiency on the X chromosome, *Df(1)NP5* (Mitchell et al., 1996). Like *fra* mutant embryos, *Netrin* mutant embryos have fewer commissural axons, with those in the posterior commissure being most affected (Mitchell et al., 1996). As observed for *fra*, both *Abl* and *trio* dominantly enhanced the *Netrin* deficiency phenotypes and increased the frequency of defects in both commissures (Fig. 1P-R, and data not shown). In $Df(1)NP5/Y;Abl^4/+$ embryos, 33% of segments had thin or missing commissures, versus only 24% in *Df(1)NP5/Y* hemizygotes; in

Df(1)NP5/Y;trio$^{IMP159.4}$/+ embryos, 56% of segments had thin or missing commissures (Tables 1, 2; Fig. 1P-R). Genetic interactions of *Abl* and *trio* with the *Netrin* genes further support the idea that *Abl* and *trio* are required to attract growth cones to the CNS midline.

Although mutations in *Abl* and *trio* dominantly enhanced the loss-of-commissure phenotype in *fra* and *Netrin* mutants, we did not observe other dose-sensitive interactions between *fra*, *Abl* and *trio*. For example, mutations in *fra* did not reciprocally enhance the loss-of-commissure phenotype in *Abl* or *trio* mutants, although the percentage of segments with axon pathfinding errors increased when one dose of *fra* was removed in the *Abl* mutant background (Tables 1, 2; Fig. 1I,J). We also did not observe transheterozygous interactions between *Abl*, *trio* and *fra* in single, double and triple transheterozygous mutant combinations. In all of these cases, no more than 5% of segments had disrupted commissures (Table 3, Fig. 1K). Furthermore, even in embryos that were homozygous mutant for one of these three genes, heterozygosity for the two remaining genes did not lead to additive or synergistic increases in commissure defects (Table 3). Because in other experiments, *Abl* and *trio* behaved genetically as *fra* effectors (see below), the inability of *fra* to dominantly enhance *Abl* or *trio* loss-of-commissure defects, and the lack of transheterozygous interactions between *fra*, *Abl* and *trio*, may be due to the presence of maternally-contributed *Abl* and *trio* in the embryo (Bennett and Hoffmann, 1992; Liebl et al., 2000; Wadsworth et al., 1985). Another possibility is that heterozygosity for *fra* simply does not reduce the effective dose enough to enhance *Abl* or *trio* loss-of-commissure phenotypes.

Table 3. *fra*, *Abl* and *trio* do not interact transheterozygously

Genotype	% Defective segments, overall (*n*)	% Segments with thin/ missing commissures	% Segments with path-finding errors
fra^{4}/+	1.9 (209)	0	1.9
Abl^{1}/+	1.8 (217)	0	1.8
trio$^{IMP159.4}$/+	0.9 (218)	0	0.9
fra^{4}/+;*Abl*^{1}/+	1.5 (205)	0	1.5
fra^{4}/+;*trio*$^{IMP159.4}$/+	4.3 (208)	2.4	1.9
trio$^{IMP159.4}$,+/+,*Abl*^{1}	1.4 (211)	0	1.4
Df(2R)vg135/+;Df(3L)FpaI,Abl^{4}/+,+	0.5 (191)	0	0.5
fra^{4}/+;*trio*$^{IMP159.4}$,+/+,*Abl*^{1}	3.3 (212)	0	3.3
fra^{4}/*fra*^{4}	36 (212)	23	13
fra^{4}/*fra*^{4};*Abl*^{4}/+	45 (458)	33	12
fra^{4}/*fra*^{4};*trio*$^{P0368/10}$/+	69 (162)	47	22
fra^{4}/*fra*^{4};*trio*$^{IMP159.4}$/+	90 (213)	80	10
fra^{4}/*fra*^{4};*trio*$^{P0368/10}$,+/+,*Abl*^{4}	66 (196)	60	6
fra^{4}/*fra*^{4};*trio*$^{IMP159.4}$,+/+,*Abl*^{4}	88 (140)	76	12
Abl^{4}/*Abl*^{1}	6.6 (257)	1.2	5.4
fra^{4}/+;*Abl*^{4}/*Abl*^{1}	11.8 (286)	1.0	10.8
Df(3L)FpaI,Abl^{4}/+,*Abl*^{1}	31 (227)	12	19
fra^{4}/+;*Df(3L)FpaI,Abl*^{4}/+,*Abl*^{1}	28 (235)	8	20
trio$^{IMP159.4}$/*Df(3L)FpaI*	6.4 (421)	1.9	4.5
fra^{4}/+;*trio*$^{IMP159.4}$/*Df(3L)FpaI*	3.3 (216)	0.5	2.8
trio$^{IMP159.4}$,+/*Df(3L)FpaI,Abl*^{4}	22 (212)	10	12
fra^{4}/+;*trio*$^{IMP159.4}$,+/*Df(3L)FpaI,Abl*^{4}	16 (220)	3	13

For single transheterozygous combinations, crosses were performed at 25°C. All other crosses were conducted at room temperature (22°C).
Percentages were not rounded when overall defects were less than 15%.

Commissure formation is severely disrupted in double mutant *fra;Abl* and *fra;trio* embryos

As in *trio,Abl* double mutant embryos, *fra;Abl* and *fra;trio* double mutant embryos had severe CNS phenotypes in which the majority of segments had thin or missing commissures. In *fra*^{4}*/Df(2R)vg135;Abl*^{4}*/Abl*^{1} embryos, 85% of segments had thin or missing commissures (Fig. 1L,M; Table 1). In *fra*^{4}*/Df(2R)vg135;trio*$^{IMP159.4}$*/trio*^{M89} embryos, 66% of segments had thin/missing commissures (Fig. 1N,O; Table 2). In these animals, as in homozygous *fra*, heterozygous *Abl* or *trio* mutants, the posterior commissure was affected more often than the anterior commissure. For example, in *fra*^{4}*/Df(2R)vg135;Abl*^{4}*/Abl*^{1} embryos, 79% of posterior commissures were thin/missing, versus only 49% of anterior commissures (*n*=166 segments); in *fra*^{4}*/Df(2R)vg135; trio*$^{IMP159.4}$*/trio*^{M89} embryos, 62% of posterior commissures were thin/missing, versus only 33% of anterior commissures (*n*=172 segments).

Additionally, although there were occasional breaks (>75% of axons missing) in longitudinal connectives in *fra* homozygotes [10% (*n*=519) in *fra*^{4}*/Df(2R)vg135* embryos], in *fra;Abl* and *fra;trio* double mutants this type of defect did not increase considerably. For example, only 11% (*n*=387) of connectives had breaks in *fra*^{4}*/Df(2R)vg135;Abl*^{4}*/Abl*^{1} embryos, and 16% (*n*=368) in *fra*^{4}*/Df(2R)vg135;trio*$^{IMP159.4}$*/ trio*^{M89} embryos. However, analysis of subsets of longitudinally-projecting axons in stage 17 embryos using the monoclonal antibody 1D4 (anti-Fasciclin II) revealed a significant disorganization of these pathways, especially in *fra;Abl* double mutants (see Fig. S1 and Table S1 in the supplementary material). In *fra;Abl* and *fra;trio* double mutants, Fas2-positive longitudinal pathways wandered medially or laterally, often seeming to intertwine so that individual bundles were indistinguishable. In addition, although breaks in all three longitudinal bundles between segments were rare, often one to two (usually lateral) 1D4-positive bundles were discontinuous between segments. Similar defects were observed at a lower frequency in individual *fra*, *Netrin*, *Abl* and *trio* mutants (see Fig. S1 and Table S1 in the supplementary material). Thus, although BP102 immunohistochemistry did not reveal consistent defects in longitudinal pathways, the disorganization of Fas2-positive axon bundles suggests that Fra, Abl and Trio function during axon pathfinding in longitudinal pathways in addition to their roles during commissure formation.

Mutations in *enabled* suppress *frazzled*, *Netrin* and *trio,Abl* CNS phenotypes

In the CNS, *ena* interacts genetically with the repulsive receptor *robo*, leading to inappropriate crossing of the midline by longitudinal axons (Bashaw et al., 2000). In *Abl*, *trio* and *fra* mutant combinations, numerous axons fail to cross the midline (Liebl et al., 2000) (Tables 1, 2). We explored this apparently antagonistic relationship further by analyzing genetic interactions among *trio*, *Abl*, *fra*, the *Netrin* genes and *ena* in the CNS.

Mutations in *ena* dominantly reduced the severity of the CNS phenotype in *trio,Abl* mutants. For example, in *ena* heterozygous, *trio,Abl* homozygous (*ena*^{GC10}/+;*trio*^{M89},*Abl*^{1}/

Df(3L)FpaI,Abl^{4}) embryos, only 78% of segments had defective commissures, versus 100% in the *trio,Abl* (*trio*^{M89},*Abl*^{1}/*Df(3L)FpaI,Abl*^{4}) double mutant (Table 4; and compare Fig. 1D,E with 1T). Overall, there was a 20% reduction in the number of segments with thin or missing commissures (Table 4). However, analysis of individual commissures revealed a dramatic increase in the number of axons which crossed the midline when compared with the *trio,Abl* double mutant, especially in the anterior commissure. For example, in *ena* heterozygous, *trio,Abl* homozygous (*ena*^{GC10}/+;*trio*^{M89},*Abl*^{1}/*Df(3L)FpaI,Abl*^{4}) embryos, only 24% of anterior commissures and 59% of posterior commissures were thin or missing (*n*=206 segments), compared with 64% of anterior commissures and 84% of posterior commissures in *trio,Abl* embryos (*n*=160 segments) (Fig. 1D,E,T). In another mutant combination, the increase in the number of axons crossing the midline was even more striking. In *Df(3L)FpaI,Abl*^{4}/*trio*$^{IMP159.4}$,*Abl*^{1} embryos, 65% of segments had thin or missing commissures, whereas in *ena*^{GC5}/+;*Df(3L)FpaI,Abl*^{4}/*trio*$^{IMP159.4}$,*Abl*^{1} embryos only 9% of segment commissures were thin or missing (Table 4). Removing one dose of *ena* in the *trio,Abl* homozygous mutant background also decreased the number of breaks in longitudinal connectives (Fig. 1D,E,T; and see Table S1 in the supplementary material).

Mutations in *ena* also dominantly suppressed CNS defects in *fra* and *Netrin* mutants. For example, in *Df(1)NP5/Y;ena*^{GC10}/+ embryos, only 7% of segments had thin/missing commissures, versus 24% in *Df(1)NP5/Y* embryos (Fig. 1P,S, and Table 4). In *fra*^{4},*ena*^{GC10}/*Df(2R)vg135* embryos, 10% of segments had thin or missing commissures, versus 13% in *fra*^{4}/*Df(2R)vg135* animals (Table 4).

Table 4. Heterozygosity for *ena* dominantly suppresses commissure defects in *fra*, *Netrin* and *trio,Abl* mutant embryos

Genotype	% Defective segments, overall (*n*)	% Segments with thin/ missing commissures	% Segments with path-finding errors
trio^{M89},*Abl*^{1}/*Df(3L)FpaI,Abl*^{4}	100 (160)	86	14
ena^{GC10}/+;*trio*^{M89},*Abl*^{1}/*Df(3L)FpaI, Abl*^{4}	78 (206)	65	13
Df(3L)FpaI,Abl^{4}/*trio*$^{IMP159.4}$,*Abl*^{1}	85 (196)	65	20
ena^{GC5}/+;*Df(3L)FpaI,Abl*^{4}/*trio*$^{IMP159.4}$, *Abl*^{1}	29 (208)	9	20
fra^{4}/*Df(2R)vg135*	21 (1279)	13	8
fra^{4},*ena*^{GC10}/*Df(2R)vg135*	17 (799)	10	7
Df(1)NP5/Y	34 (277)	24	10
Df(1)NP5/Y;ena^{GC10}/+	17 (308)	7	10
Df(1)NP5/Y;ena^{210}/+	26 (222)	11	15
Df(1)NP5/Y;ena^{23}/+	20 (212)	13	7
fra^{4}/*fra*^{4}	36 (212)	23	13
fra^{4}/*fra*^{4};*Abl*^{4}/+	45 (458)	33	12
fra^{4},*ena*^{GC10}/*fra*^{4};*Abl*^{4}/+	26 (221)	14	12
fra^{4}/*fra*^{4};*trio*$^{IMP159.4}$/+	90 (213)	80	10
fra^{4},*ena*^{GC10}/*fra*^{4};*trio*$^{IMP159.4}$/+	25 (197)	15	10

Percentages were not rounded when overall defects were less than 15%.

Heterozygosity for *ena* also suppressed enhancement of the *fra* CNS phenotype by *Abl* or *trio*. For example, in *fra*^{4},*ena*^{GC10}/*fra*^{4};*Abl*^{4}/+ embryos 14% of segments had thin/missing commissures, versus 33% in *fra*^{4}/*fra*^{4};*Abl*^{4}/+ mutants, and 23% in *fra*^{4}/*fra*^{4} embryos. Similarly, in *fra*^{4}/*fra*^{4};*trio*$^{IMP159.4}$/+ embryos, 80% of segments had thin or missing commissures, compared with only 15% in *fra*^{4},*ena*^{GC10}/*fra*^{4};*trio*$^{IMP159.4}$/+ embryos (Table 4).

Heterozygosity for *Abl*, *trio* and *ena* suppresses inappropriate midline crossing by axons expressing the chimeric Robo-Fra receptor

The genetic interactions described support roles for Abl, Trio and Ena during commissure formation, but these types of interactions (dominant enhancement/suppression and synergistic double mutant genetic interactions) are usually interpreted to mean that gene products function in parallel pathways; it is likely, for example, that Abl and Trio are instructed by at least one other receptor that positively regulates commissure formation. To test genetically whether Abl, Trio and/or Ena might function as Fra effector(s) in vivo, we took advantage of the fact that neuronal expression of a chimeric receptor composed of the extracellular and transmembrane domains of the repulsive Robo receptor and the intracellular domain of Fra causes CNS axons to inappropriately sense the midline-secreted repellent Slit as an attractant and cross the midline boundary inappropriately (Bashaw and Goodman, 1999). If Abl, Trio and/or Ena function as effectors of Fra signaling in axons that cross the midline, then reducing the dose of these molecules genetically would be expected to reduce the severity of the chimeric Robo-Fra receptor phenotype. We chose this strategy because, in the *Drosophila* embryo, overexpressing full-length Fra in CNS neurons does not cause robust ectopic midline crossing by CNS axons (D.J.F. and P.A.K., unpublished) (Kim et al., 2002).

In wild-type stage 17 embryos, Fas2-positive axons project longitudinally in three bundles on either side of the midline, but these axons never cross the midline boundary (Fig. 2A). In embryos expressing UAS-Robo-Fra in all neurons, numerous Fas2-positive axon bundles crossed the midline inappropriately (Table 5, Fig. 2B). Reducing the gene dose of *Abl* in embryos expressing the chimeric receptor led to a moderate reduction in the number of these ectopic crossovers (Table 5). Similarly, in three out of four alleles tested, heterozygosity for *trio* also reduced the severity of the Robo-Fra phenotype (Table 5). In these experiments, the deficiency *Df(3L)FpaI* suppressed the Robo-Fra receptor phenotype most strongly, and not the imprecise excision allele *trio*$^{IMP159.4}$, which acted as the strongest dominant enhancer of the *fra* loss-of-function phenotype (Table 2). It is possible that other, unidentified genes removed by the FpaI deficiency also function as Fra effectors, that the other *trio* alleles encode Trio proteins that retain partial function downstream of Fra signaling, or that *trio*$^{IMP159.4}$ disrupts signaling by other receptor(s) that mediate commissure formation more strongly than this allele interferes with Fra signaling. We also discovered that if the *Df(3L)FpaI* chromosome was contributed to progeny by the male parent, rather than the female, genetic suppression of the Robo-Fra phenotype was less severe (Table 5), suggesting that maternal contribution of *trio* (or another gene removed by this deficiency) plays a role.

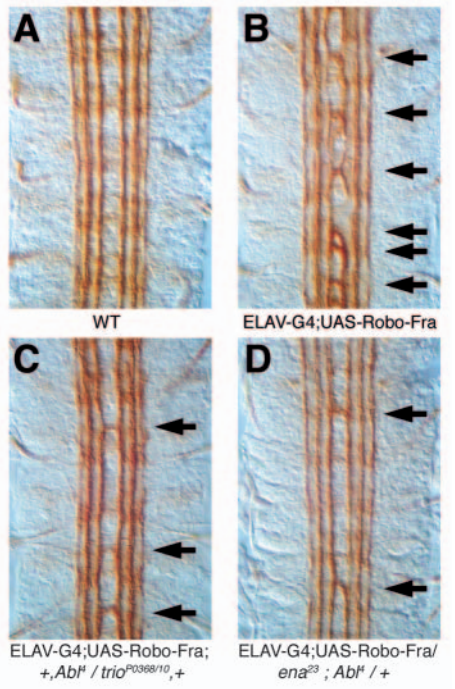

Fig. 2. Heterozygosity for *Abl*, *trio* and *ena* reduces the severity of inappropriate midline crossing by axons expressing the chimeric Robo-Fra receptor. A subset of longitudinally projecting axons in stage 17 embryos were labeled with mAb 1D4 (anti-Fas2). Examples of Fas2-positive bundles scored as ectopic crossovers are indicated with arrows. (A) In wild-type embryos, Fas2-positive axons project in three distinct longitudinal bundles on either side of the CNS midline, but never cross the midline. (B) In embryos expressing UAS-Robo-Fra under the control of the ELAV-GAL4 postmitotic neuronal driver, numerous Fas2-positive axon bundles cross the midline, reflecting inappropriate attraction towards the midline repellent Slit. (C) In embryos heterozygous for *Abl* and *trio*, fewer axon bundles cross the midline. (D) Heterozygosity for *Abl* and *ena* also reduces the severity of the Robo-Fra phenotype.

Interestingly, although heterozygosity for Abl^4 [the *Abl* point mutant allele thought to be protein-null or nearly null (Bennett and Hoffmann, 1992)] led to a negligible reduction in ectopic crossovers on its own (0.84 crossovers/segment), heterozygosity for this allele of *Abl* and three different *trio* mutations led to a moderately synergistic reduction in the number of inappropriate crossovers. For example, in ELAV-GAL4; UAS-Robo-Fra; $+,Abl^4/trio^{P0368/10}/+$ embryos, only 0.47 axon bundles per segment crossed the midline inappropriately, compared with 0.61 crossovers/segment in ELAV-GAL4; UAS-Robo-Fra; $trio^{P0368/10}/+$ embryos (Table 5, Fig. 2C). These data are consistent with positive roles for both Abl and Trio as effectors of Fra signaling in axons that cross the CNS midline.

Heterozygosity for three different alleles of *ena* also reduced the severity of the Robo-Fra phenotype (Table 5). Furthermore, reducing the gene dose of both *Abl* and *ena* also led to a synergistic reduction in the number of ectopic midline crossovers by Fas2-positive axons, similar to the genetic interaction between *Abl* and *trio* in embryos expressing Robo-Fra. For example, in ELAV-GAL4; UAS-Robo-Fra/ena^{23}; $Abl^4/+$ embryos, there were only 0.23 crossovers per segment, compared with 0.47 crossovers/segment in Robo-Fra-

Table 5. Heterozygosity for *Abl*, *trio* and *ena* genetically suppresses ectopic midline crossing by axons expressing the Robo-Fra chimeric receptor

Genotype	Crossovers/segment* (*n*)	Penetrance† (*n*)	Expressivity‡ (defects/embryo)
ELAV-G4; UAS-Robo-Fra	0.86 (261)	100% (24)	9.3
ELAV-G4; UAS-Robo-Fra; $Abl^4/+$	0.84 (242)	100% (22)	9.2
ELAV-G4; UAS-Robo-Fra; $Abl^1/+$	0.78 (183)	100% (17)	8.5
ELAV-G4; UAS-Robo-Fra; *Df(3L)st-j7*/+	0.74 (247)	100% (21)	8.8
ELAV-G4; UAS-Robo-Fra; $trio^{M89}/+$	0.88 (217)	100% (19)	10.1
ELAV-G4; UAS-Robo-Fra; $trio^{P0368/10}/+$	0.61 (241)	100% (22)	6.8
ELAV-G4; UAS-Robo-Fra; $trio^{IMP159.4}/+$	0.65 (242)	96% (22)	7.5
ELAV-G4; UAS-Robo-Fra; *Df(3L)FpaI*/+§	0.39 (229)	57% (21)	7.5
ELAV-G4; UAS-Robo-Fra; *Df(3L)FpaI(MALE)*/+¶	0.62 (95)	100% (8)	7.4
ELAV-G4; UAS-Robo-Fra; $+,Abl^4/trio^{M89},+$	0.78 (302)	100% (26)	9.0
ELAV-G4; UAS-Robo-Fra; $+,Abl^4/trio^{P0368/10},+$	0.47 (176)	100% (15)	5.5
ELAV-G4; UAS-Robo-Fra; *Df(3L)FpaI*,Abl^4/+,+	0.28 (318)	79% (29)	3.9
ELAV-G4; UAS-Robo-Fra/ena^{GC10}	0.65 (246)	100% (23)	6.9
ELAV-G4; UAS-Robo-Fra/ena^{23}	0.47 (201)	88% (17)	6.3
ELAV-G4; UAS-Robo-Fra/ena^{210}	0.59 (257)	96% (22)	7.2
ELAV-G4; UAS-Robo-Fra/ena^{GC10}; $Abl^4/+$	0.35 (172)	81% (16)	4.6
ELAV-G4; UAS-Robo-Fra/ena^{23}; $Abl^4/+$	0.23 (223)	74% (19)	3.6

Stage 17 embryos were stained with mAb 1D4 and dissected. At least nine segments/embryo were scored for Fas2-positive axon bundles that crossed the midline inappropriately.

*Because some segments had two crossovers, the 'crossovers/segment' score is the total number of crossovers divided by total number of segments (*n*) scored for that genotype.

†Penetrance is the number of embryos with defects divided by the total number (*n*) of embryos scored.

‡Expressivity is the total number of ectopic crossovers divided by the number of affected embryos.

The same UAS-Robo-Fra transgenic chromosome ('3.1') was used in each cross.

§In these embryos, the *Df(3L)FpaI* chromsome was contributed by the female parent.

¶The *Df(3L)FpaI* chromsome was contributed by the male parent.

expressing embryos heterozygous for *ena*^{23} only (Table 5, Fig. 2D). While these data were initially surprising because heterozygosity for *ena* led to an increase in the number of axons that crossed the midline in *fra*, *Netrin*, *Abl* and *trio* loss-of-function mutants (Table 4), they are consistent with the idea that Ena may be functioning positively as an effector of signaling via the Fra cytoplasmic domain, similar to orthologs of Ena in other organisms (see Discussion) (see also Gitai et al., 2003; Lebrand et al., 2004).

Physical interactions between Fra, Abl and Trio

To test whether Fra could physically interact with Abl, Trio or Ena, we first asked whether glutathione-S-transferase (GST) fusions with the cytoplasmic domain of Fra (generated in *E. coli*) could bind in vitro translated Abl, Trio or Ena. In these experiments, Abl and Trio, but not Ena, specifically bound GST-Fra$_{CYTO}$, but not GST or glutathione beads alone (Fig. 3A and data not shown), indicating that the cytoplasmic domain of Fra can interact directly with Abl and Trio. In parallel experiments, we also found that GST-Fra could interact with Abl-Myc and Trio-Myc in extracts from *Drosophila* Schneider-2 (S2) cells that had been engineered to express each protein (not shown).

In addition, in vitro translated Abl-Myc bound specifically to GST-TrioSH3 (Fig. 3B), and Trio-Myc bound specifically to GST-AblSH3 (Fig. 3C), indicating that Abl and Trio can interact directly as well via their SH3 domains. GST-TrioSH3 includes linker sequences on either side of the SH3 domain. Deleting most of the SH3 domain and C-terminal linker sequences in GST-TrioSH3 (L1624-L1840) abolishes Abl-Myc binding (not shown), suggesting that the SH3 domain mediates the interaction with Abl. In all of the GST-pulldown experiments, the Trio constructs used were deleted for the spectrin-like repeats in order to maximize expression level and stability (full-length, the molecular mass of wild-type Trio is greater than 225 kDa). Thus, at least in these in vitro assays, the spectrin-like repeats are not required for the interaction of Trio with either the cytoplasmic domain of Fra or the SH3 domain of Abl.

Next, we investigated whether full-length Fra could interact with full-length Abl, Trio and/or Ena in S2 cells. Hemagglutinin (HA)-tagged Fra was transiently co-expressed with either Abl-Myc, Trio-Myc or Ena, and extracts were subjected to immunoprecipitation. Fra-HA specifically co-immunoprecipitated in the presence of Abl-Myc or Trio-Myc, but not in their absence (Fig. 3D,E, lanes 1 and 2). This interaction is mediated by the cytoplasmic domain of Fra, as a Fra protein deleted for this domain did not co-immunoprecipitate with either Abl or Trio (Fig. 3D,E, lane 3). We did not observe a similar association between Ena and Fra-HA in S2 cells, using either anti-Ena or anti-HA antibodies for co-immunoprecipitation (data not shown).

Fra and Trio are tyrosine phosphorylated in S2 cells

The genetic and physical interactions that we observed among Fra, Trio and Abl raised the possibility that Fra and Trio might be substrates for the Abl tyrosine kinase. To determine whether or not phosphotyrosine could be detected on Fra or Trio, we transiently expressed full-length, epitope-tagged versions of Trio and Fra in S2 cells, and treated the cells with pervanadate, a potent phosphotyrosine phosphatase inhibitor that has been used previously to sustain tyrosine phosphorylation of proteins

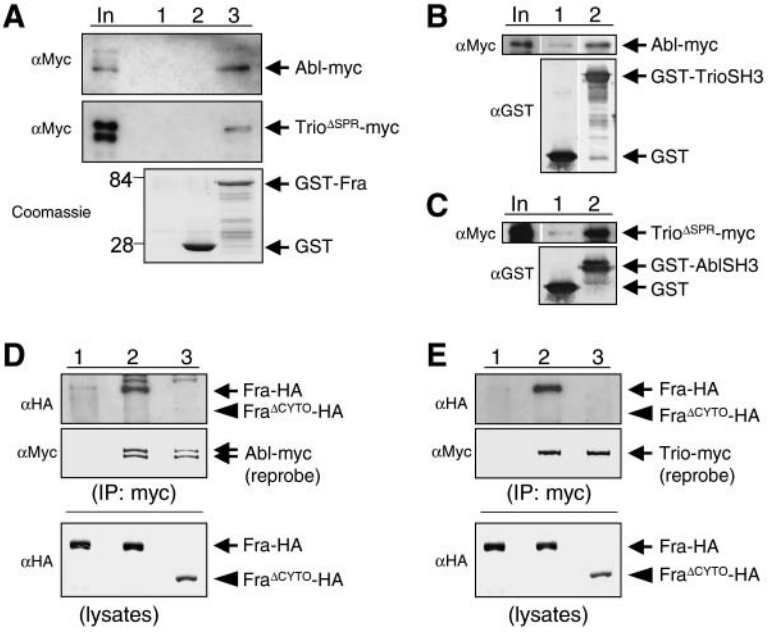

Fig. 3. Physical interactions between Fra, Abl and Trio. (A) The cytoplasmic domain of Fra interacts directly with Abl and Trio. Beads only (lane 1), GST bound to beads (lane 2) or GST-Fra$_{CYTO}$ bound to beads (lane 3) were incubated with in vitro translated, epitope-tagged Abl or Trio. Approximately 20% of each pulldown (~2 μg of fusion protein) and bound target proteins were resolved by SDS-PAGE. Bound proteins (top two blots) were visualized by anti-Myc immunoblotting, and fusion proteins (bottom gel) were visualized by Coomassie staining. 'In' represents 2% of total input protein incubated with beads, GST or GST-Fra$_{CYTO}$. Abl and Trio specifically interact with GST-Fra$_{CYTO}$ (lane 3), but not GST or beads (lanes 1 and 2). Trio$^{\Delta SPR}$-Myc is deleted for the spectrin-like repeats to optimize expression in vitro. (B,C) Trio and Abl interact directly via their SH3 domains. (B) GST-TrioSH3 (lane 2), but not GST (lane 1), specifically pulls down in vitro translated Abl-Myc. (C) GST-AblSH3 (lane 2), but not GST (lane 1), specifically pulls down in vitro translated Trio$^{\Delta SPR}$-Myc. 'In' represents ~2.5% of input incubated with GST or fusion protein. Target proteins were visualized by anti-Myc staining, whereas fusion proteins (bottom gel) were visualized by anti-GST staining. Panels B and C were assembled from different lanes on the same gel. (D,E) Fra complexes via its cytoplasmic domain with Abl and Trio in S2 cells. (D) HA-tagged Fra (arrow, lanes 1 and 2, bottom gel) or Fra$^{\Delta CYTO}$, a Fra molecule lacking the intracellular domain (arrowhead, lane 3, bottom gel), were co-expressed in S2 cells with Abl-Myc (lanes 2 and 3, middle gel), and complexes were immunoprecipitated with anti-Myc antibody. Fra-HA (arrow, top gel) co-immunoprecipitates only in the presence of Abl-Myc (compare lanes 1 and 2). Fra$^{\Delta CYTO}$-HA (arrowhead indicates the absence of Fra$^{\Delta CYTO}$-HA, top gel) does not co-immunoprecipitate with Abl-Myc (compare lanes 2 and 3). When expressed in S2 cells, Abl-Myc runs as a ~180-190 kDa doublet, similar to untagged Abl (D, compare with Fig. 4C,D). Additional low-mobility bands in D (top gel, lanes 2 and 3) are background staining of Abl-Myc, which is nearly the same size as Fra-HA. (E) Fra-HA (lane 2) but not Fra$^{\Delta CYTO}$-HA (lane 3) co-immunoprecipitates with Trio-Myc.

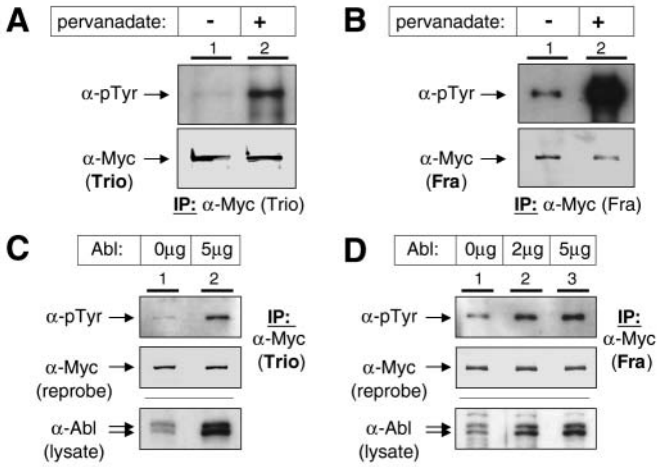

Fig. 4. Trio and Fra are tyrosine phosphorylated in S2 cells. (A,B) Pervanadate treatment results in robust elevation of phosphotyrosine levels in both Trio and Fra proteins. S2 cells transiently expressing Trio-Myc (A) or Fra-Myc (B) were mock-treated with PBS (lane 1) or treated with pervanadate (lane 2) for 30 minutes. Target proteins were immunoprecipitated, and equivalent aliquots of immune complexes were resolved by SDS-PAGE. Blots were probed with either anti-phosphotyrosine (top gel) or anti-Myc (bottom gel). (C,D) Tyrosine phosphorylation of both Trio (C, lane 2) and Fra (D, lanes 2 and 3) is elevated in the presence of increased Abl levels (top gel). S2 cells were co-transfected with 5 μg of pMET Trio-Myc (C) or pMET Fra-Myc (D) and 0, 2 or 5 μg of pMET Abl, as indicated. Twenty-four hours after induction, target proteins were immunoprecipitated and resolved via SDS-PAGE. Blots were probed with anti-phosphotyrosine (top gel), then stripped and re-probed with anti-Myc to verify equivalent loading of samples (middle gel). Approximately 2% of total lysates used in each IP were resolved separately and elevated Abl levels were verified with anti-Abl (bottom gel).

in *Drosophila* cells (Fashena and Zinn, 1997; Muda et al., 2002). In control S2 cells, Trio tyrosine phosphorylation was not detected, whereas Fra was moderately tyrosine phosphorylated (Fig. 4A,B, lane 1). After a 30-minute pervanadate treatment, both molecules were robustly tyrosine phosphorylated, indicating that Trio and Fra are substrates of tyrosine kinases and phosphatases expressed endogenously in S2 cells (Fig. 4A,B, lane 2).

Next, we investigated whether elevating Abl levels in S2 cells would increase tyrosine phosphorylation of Trio or Fra. Phosphotyrosine on Trio increased dramatically when Abl was co-expressed (Fig. 4C, lane 2). Fra was also tyrosine phosphorylated at a higher level when Abl was co-expressed, although not quite as robustly as Trio (Fig. 4D, lanes 2 and 3). We observed a similar elevation of tyrosine phosphorylation of Ena, a known Abl substrate, in S2 cells treated with pervanadate or cotransfected with Abl (not shown). These results indicate that Abl either phosphorylates Fra and Trio directly, or indirectly regulates Fra and Trio tyrosine phosphorylation.

Discussion

Recent investigations into the molecular mechanisms of axon guidance have focused on identifying which cytoplasmic molecules cooperate with which growth cone receptors to regulate actin cytoskeletal dynamics and growth cone motility (Huber et al., 2003). In this study, we present evidence that Abl, Trio and Ena function together with the Netrin receptor Fra to regulate chemoattraction to the *Drosophila* embryonic CNS midline.

We found that mutations in *Abl* and *trio* dominantly enhance the CNS phenotype in *fra* and *Netrin* mutant embryos, and that *fra;Abl* and *fra;trio* double mutants have a severe CNS phenotype in which a majority of commissures are thin or missing, similar to the *trio,Abl* double mutant phenotype. Mutations in *Abl* and *trio* reduce the number of axons that cross the midline inappropriately in embryos expressing the chimeric Robo-Fra receptor. Abl and Trio interact physically with the cytoplasmic domain of Fra, and increasing Abl kinase expression in cells increases tyrosine phosphorylation of Fra and Trio. Interpreting these data together, we conclude (1) that Abl, Trio and Fra function together during commissure formation, (2) that the severe double mutant phenotypes reflect the disruption of multiple signaling pathways or networks in the growth cones of commissural axons (i.e. Abl and Trio function downstream of at least one other receptor that positively regulates commissure formation), and (3) that the lack of other dose-sensitive interactions between *fra*, *Abl* and *trio* is a result of redundancy (other receptors/effectors mediating commissure formation), or the presence of maternally contributed proteins.

The interactions of Abl with Fra are intriguing, as they suggest that in *Drosophila*, as in other organisms, this evolutionarily conserved guidance receptor is regulated by tyrosine phosphorylation, and also that Fra may regulate Abl substrates. Recently, others have demonstrated Netrin-dependent tyrosine phosphorylation of DCC, Netrin/DCC-dependent activation of the tyrosine kinases FAK, Src and Fyn, and the requirement of DCC tyrosine phosphorylation for Netrin-dependent Rac1 activation and growth cone turning (Li et al., 2004; Liu et al., 2004; Meriane et al., 2004; Ren et al., 2004). Interestingly, the tyrosine residue in DCC identified as the principal target of Fyn/Src kinases is not conserved in *Drosophila* Fra or *C. elegans* UNC-40, suggesting that the precise mechanisms by which Fra/DCC/UNC-40 signaling is regulated by tyrosine kinases may differ between organisms (Li et al., 2004; Meriane et al., 2004). Tyrosine phosphorylation of UNC-40 has also been observed, and although the kinase(s) responsible has not been identified, genetic interactions suggest that UNC-40 signaling is regulated by the RPTP CLR-1, supporting the idea that regulation of tyrosine phosphorylation is a consequence of UNC-6/Netrin signaling in *C. elegans* as well (Chang et al., 2004; Tong et al., 2001). In this study, we observed more robust tyrosine phosphorylation of Fra in cells with pervanadate stimulation than with Abl overexpression alone, raising the possibility that additional kinase(s) may function during Fra signaling. Further investigation will be needed to address this issue and to determine how Abl-mediated phosphorylation of Fra modulates commissural growth cone guidance.

Abl is thought to control actin dynamics in part through its ability to regulate other proteins through tyrosine phosphorylation (Lanier and Gertler, 2000; Woodring et al., 2003). Thus, in addition to potential regulation of Fra, Fra may recruit Abl to regulate other Abl substrates. *Abl* interacts genetically with *trio* (Liebl et al., 2000), and in this study, we

have found that Trio physically interacts with Abl in vitro and that Trio tyrosine phosphorylation increases dramatically with co-expression of Abl. Phosphorylation of Trio may affect its activity, as observed for other GEFs. For example, Abl regulates phosphorylation and Rac-GEF activity of Sos1, and Lck, Fyn, Hck and Syk kinases tyrosine phosphorylate Vav GEF and stimulate its activity (Sini et al., 2004; Turner and Billadeau, 2002).

Trio physically interacts with Fra in vitro and in S2 cells, suggesting that Fra can recruit Trio directly. In addition, heterozygosity for *trio* dominantly modifies the Robo-Fra chimeric receptor phenotype, consistent with a positive role for Trio as a downstream effector of Fra signaling in vivo. As a Rac/Rho GEF, Trio may link Netrin-Fra signaling to the regulation of Rho-family GTPases in commissural axons. Rho-family GTPases have been rigorously studied with regard to their role in the regulation of cytoskeletal dynamics and axon guidance, outgrowth and branching (Dickson, 2001; Luo, 2000). Although positive roles for GTPases in commissure formation in the *Drosophila* embryo have not been directly demonstrated, *trio* (in this study) and *GEF64C*, a Rho GEF (Bashaw et al., 2001), interact genetically with *fra* leading to the dramatic disruption of commissures. Additionally, expression of constitutively active or dominantly negative isoforms of both Rac and Rho, as well as constitutively active Cdc42, causes axons to cross the CNS midline inappropriately (Fan et al., 2003; Fritz and VanBerkum, 2002; Matsuura et al., 2004). Recent studies have implicated Cdc42 and Rac1/CED-10 as effectors of DCC and UNC-40 signaling, but the biochemical mechanisms by which GTPases are regulated have been elusive (Gitai et al., 2003; Li et al., 2002a; Li et al., 2002b; Shekarabi and Kennedy, 2002). Future experiments must determine whether Netrin-Fra signaling modulates the GEF activity of Trio, and how this occurs.

In this study, we found that reducing the genetic dose of *ena* causes either more or fewer axons to cross the CNS midline, depending on the genetic background, suggesting that the role of Ena in the growth cone is complex. Heterozygosity for *ena* in embryos expressing the Robo-Fra chimeric receptor reduces the number of axon bundles that inappropriately cross the CNS midline, consistent with a role for Ena as a positive effector of Fra signaling. Ena/UNC-34 has been identified genetically as an effector of DCC/UNC-40 in *C. elegans* (Gitai et al., 2003). In cultured mouse neurons, Ena/VASP proteins are required for Netrin-DCC-dependent filopodia formation, and Mena is phosphorylated at a PKA regulatory site in response to Netrin stimulation (Lebrand et al., 2004). In migrating fibroblasts, increasing Ena/VASP proteins at the leading edge leads to unstable lamellae and decreased motility; by contrast, increasing Ena/VASP levels at the leading edge in growth cones causes filopodia formation, possibly due to differences in the distribution of actin bundling or branching proteins (Bear et al., 2000; Bear et al., 2002; Lebrand et al., 2004). Although the role of Ena in actin reorganization in *Drosophila* has not been rigorously studied, Ena localizes to filopodia tips in cultured *Drosophila* cells, suggesting that the role of Ena in filopodia formation may be conserved (Biyasheva et al., 2004).

We have not observed a direct biochemical interaction between Fra and Ena. However, Abl binds and phosphorylates Ena, and heterozygosity for both *Abl* and *ena* further suppresses the Robo-Fra phenotype, suggesting that Fra may recruit Abl to regulate filopodial extension through Ena (Comer et al., 1998; Gertler et al., 1995). Alternatively, Fra may regulate Ena through other molecule(s), and the synergistic suppression of the Robo-Fra phenotype by *Abl* and *ena* is a result of the compromise of parallel pathway(s) regulated by Fra. It is important to note that the functional consequences of biochemical interactions between Abl and Ena are not understood (Comer et al., 1998; Grevengoed et al., 2003; Krause et al., 2003). Therefore it will be of particular interest to determine whether Ena is tyrosine phosphorylated in response to Netrin-Fra signaling, and if Ena phosphorylation regulates its activity during filopodial extension.

In addition to suppressing the Robo-Fra chimeric receptor phenotype, mutations in *ena* also suppress the loss-of-commissure phenotype in *fra*, *Netrin*, *trio* and *Abl* mutant combinations. In *Drosophila* (as well as in *C. elegans*), Ena interacts genetically and biochemically with the repulsive receptor Robo, indicating that Ena may restrict axon crossing at the midline (Bashaw et al., 2000; Yu et al., 2002). Thus, the fact that mutations in *ena* dominantly suppress *fra*, *Netrin*, *trio* and *Abl* CNS phenotypes could simply reflect the compromise of a parallel, opposing signaling pathway. Consistent with this idea, some axons that cross the midline in *ena* heterozygous, *trio,Abl* homozygous embryos are Fas2 positive (D.J.F., unpublished), indicating a partial reduction in repulsive signaling. However, *ena* also dominantly suppresses *fra* and *Netrin* commissural pathfinding defects, without causing longitudinal Fas2-positive axons to cross the midline (D.J.F., unpublished). Reductions in Robo signaling therefore may not fully explain the ability of *ena* to suppress defects in *fra*, *Netrin*, *Abl* and *trio* mutants.

Based on the fact that mutations in *ena* suppress a number of *Abl* mutant phenotypes, it has been proposed that Abl antagonizes Ena function (Grevengoed et al., 2003; Grevengoed et al., 2001; Lanier and Gertler, 2000). In *Abl* mutant embryos, Ena and actin mislocalize during dorsal closure and cellularization, and apical microvilli are abnormally elongated, indicating that Abl regulates the localization of Ena (Grevengoed et al., 2003; Grevengoed et al., 2001). In migrating fibroblasts, increasing Ena/VASP levels at the leading edge results in long, unbranched actin filaments, unstable lamellae, and decreased motility due to increased antagonism of capping protein (Bear et al., 2000; Bear et al., 2002). Interestingly, mutations in the gene encoding *Drosophila* capping protein β enhance CNS axon pathfinding defects in *Abl* mutants, including commissure formation (Grevengoed et al., 2003). Therefore, if Fra and/or Abl regulate Ena localization in commissural axons, then in *fra*, *Netrin* or *Abl* mutants, Ena may be mislocalized in the growth cone, leading to inappropriate inhibition of capping protein and excessive F-actin filament elongation. Additionally, reducing regulation of Ena by Fra or Abl may also allow greater Ena regulation by Slit-Robo signaling. In either case, reducing the gene dose of *ena* in *fra*, *Netrin* and *trio,Abl* mutant embryos would partially relieve these effects, allowing axons to respond more efficiently to other cues and cross the midline, as we observed. Consistent with this idea, Lebrand et al. (Lebrand et al., 2004) found that either increasing or decreasing Ena/VASP proteins at the leading edge impaired the elaboration of growth cone filopodia in response to Netrin-DCC signaling, suggesting

that Ena/VASP levels must be tightly regulated in order for the growth cone to respond optimally to extracellular signals.

The role of Abl in the growth cone is also likely to be complex. Our observations implicate Abl as an effector of attractive Fra signaling. In addition, tyrosine phosphorylation of Robo by Abl is thought to negatively regulate repulsive signaling by Robo (Bashaw et al., 2000). Paradoxically though, loss-of-function mutations in *Abl*, *robo* and *slit* interact genetically, resulting in inappropriate axon crossing at the midline, and indicating that Abl may also promote repulsion in longitudinally migrating growth cones (Hsouna et al., 2003; Wills et al., 2002). Obviously, much remains to be understood about the molecular basis for genetic interactions of *Abl*, particularly how Abl and its various substrates cooperate with different growth cone receptors to yield specific cytoskeletal outputs.

In summary, we have observed genetic and biochemical interactions indicating that Abl, Trio and Ena are integrated into a complex signaling network with Fra and the Netrins during commissure formation. These observations identify another receptor that acts through these effectors, and provide a framework for further investigation of signaling by this key, evolutionarily conserved guidance receptor.

We are grateful to Drs Francis Fogerty, Greg Bashaw, Allen Comer and F. Michael Hoffmann for their kind gifts of fly stocks, antibodies and cDNA. We thank Dr Anthony Harrington and Dr Sung Ok Yoon for technical advice with biochemical experiments. We thank an anonymous reviewer for suggesting an analysis of genetic interactions with the Robo-Fra chimeric receptor. This work was supported by National Science Foundation Grant IBN-0090239 to M.A.S. and E.C.L., and by National Institutes of Health grant NS32839 to M.A.S.

Supplementary material

Supplementary material for this article is available at
http://dev.biologists.org/cgi/content/full/132/8/1983/DC1

References

Araujo, S. J. and Tear, G. (2003). Axon guidance mechanisms and molecules: lessons from invertebrates. *Nat. Rev. Neurosci.* **4**, 910-922.

Awasaki, T., Saito, M., Sone, M., Suzuki, E., Sakai, R., Ito, K. and Hama, C. (2000). The Drosophila trio plays an essential role in patterning of axons by regulating their directional extension. *Neuron* **26**, 119-131.

Bashaw, G. J. and Goodman, C. S. (1999). Chimeric axon guidance receptors: the cytoplasmic domains of slit and netrin receptors specify attraction versus repulsion. *Cell* **97**, 917-926.

Bashaw, G. J., Kidd, T., Murray, D., Pawson, T. and Goodman, C. S. (2000). Repulsive axon guidance: Abelson and Enabled play opposing roles downstream of the roundabout receptor. *Cell* **101**, 703-715.

Bashaw, G. J., Hu, H., Nobes, C. D. and Goodman, C. S. (2001). A novel Dbl family RhoGEF promotes Rho-dependent axon attraction to the central nervous system midline in Drosophila and overcomes Robo repulsion. *J. Cell Biol.* **155**, 1117-1122.

Bateman, J., Shu, H. and Van Vactor, D. (2000). The guanine nucleotide exchange factor trio mediates axonal development in the Drosophila embryo. *Neuron* **26**, 93-106.

Bateman, J. and Van Vactor, D. (2001). The Trio family of guanine-nucleotide-exchange factors: regulators of axon guidance. *J. Cell Sci.* **114**, 1973-1980.

Battye, R., Stevens, A. and Jacobs, J. R. (1999). Axon repulsion from the midline of the Drosophila CNS requires slit function. *Development* **126**, 2475-2481.

Bear, J. E., Loureiro, J. J., Libova, I., Fassler, R., Wehland, J. and Gertler, F. B. (2000). Negative regulation of fibroblast motility by Ena/VASP proteins. *Cell* **101**, 717-728.

Bear, J. E., Svitkina, T. M., Krause, M., Schafer, D. A., Loureiro, J. J., Strasser, G. A., Maly, I. V., Chaga, O. Y., Cooper, J. A., Borisy, G. G. et al. (2002). Antagonism between Ena/VASP proteins and actin filament capping regulates fibroblast motility. *Cell* **109**, 509-521.

Bennett, R. L. and Hoffmann, F. M. (1992). Increased levels of the *Drosophila* Abelson tyrosine kinase in nerves and muscles: subcellular localization and mutant phenotypes imply a role in cell-cell interactions. *Development* **116**, 953-966.

Biyasheva, A., Svitkina, T., Kunda, P., Baum, B. and Borisy, G. (2004). Cascade pathway of filopodia formation downstream of SCAR. *J. Cell Sci.* **117**, 837-848.

Chan, S. S., Zheng, H., Su, M. W., Wilk, R., Killeen, M. T., Hedgecock, E. M. and Culotti, J. G. (1996). UNC-40, a C. elegans homolog of DCC (Deleted in Colorectal Cancer), is required in motile cells responding to UNC-6 netrin cues. *Cell* **87**, 187-195.

Chang, C., Yu, T. W., Bargmann, C. I. and Tessier-Lavigne, M. (2004). Inhibition of netrin-mediated axon attraction by a receptor protein tyrosine phosphatase. *Science* **305**, 103-106.

Comer, A. R., Ahern-Djamali, S. M., Juang, J. L., Jackson, P. D. and Hoffmann, F. M. (1998). Phosphorylation of Enabled by the Drosophila Abelson tyrosine kinase regulates the in vivo function and protein-protein interactions of Enabled. *Mol. Cell. Biol.* **18**, 152-160.

Crowner, D., Le Gall, M., Gates, M. A. and Giniger, E. (2003). Notch steers Drosophila ISNb motor axons by regulating the Abl signaling pathway. *Curr. Biol.* **13**, 967-972.

Dent, E. W. and Gertler, F. B. (2003). Cytoskeletal dynamics and transport in growth cone motility and axon guidance. *Neuron* **40**, 209-227.

Dickson, B. J. (2001). Rho GTPases in growth cone guidance. *Curr. Opin. Neurobiol.* **11**, 103-110.

Eden, S., Rohatgi, R., Podtelejnikov, A. V., Mann, M. and Kirschner, M. W. (2002). Mechanism of regulation of WAVE1-induced actin nucleation by Rac1 and Nck. *Nature* **418**, 790-793.

Estrach, S., Schmidt, S., Diriong, S., Penna, A., Blangy, A., Fort, P. and Debant, A. (2002). The Human Rho-GEF trio and its target GTPase RhoG are involved in the NGF pathway, leading to neurite outgrowth. *Curr. Biol.* **12**, 307-312.

Fan, X., Labrador, J. P., Hing, H. and Bashaw, G. J. (2003). Slit stimulation recruits Dock and Pak to the roundabout receptor and increases Rac activity to regulate axon repulsion at the CNS midline. *Neuron* **40**, 113-127.

Fashena, S. J. and Zinn, K. (1997). Transmembrane glycoprotein gp150 is a substrate for receptor tyrosine phosphatase DPTP10D in Drosophila cells. *Mol. Cell. Biol.* **17**, 6859-6867.

Fritz, J. L. and VanBerkum, M. F. (2002). Regulation of rho family GTPases is required to prevent axons from crossing the midline. *Dev. Biol.* **252**, 46-58.

Gertler, F. B., Bennett, R. L., Clark, M. J. and Hoffmann, F. M. (1989). Drosophila abl tyrosine kinase in embryonic CNS axons: a role in axonogenesis is revealed through dosage-sensitive interactions with disabled. *Cell* **58**, 103-113.

Gertler, F. B., Comer, A. R., Juang, J. L., Ahern, S. M., Clark, M. J., Liebl, E. C. and Hoffmann, F. M. (1995). enabled, a dosage-sensitive suppressor of mutations in the Drosophila Abl tyrosine kinase, encodes an Abl substrate with SH3 domain-binding properties. *Genes Dev.* **9**, 521-533.

Gitai, Z., Yu, T. W., Lundquist, E. A., Tessier-Lavigne, M. and Bargmann, C. I. (2003). The netrin receptor UNC-40/DCC stimulates axon attraction and outgrowth through enabled and, in parallel, Rac and UNC-115/AbLIM. *Neuron* **37**, 53-65.

Grevengoed, E. E., Loureiro, J. J., Jesse, T. L. and Peifer, M. (2001). Abelson kinase regulates epithelial morphogenesis in Drosophila. *J. Cell Biol.* **155**, 1185-1198.

Grevengoed, E. E., Fox, D. T., Gates, J. and Peifer, M. (2003). Balancing different types of actin polymerization at distinct sites: roles for Abelson kinase and Enabled. *J. Cell Biol.* **163**, 1267-1279.

Guan, K. L. and Rao, Y. (2003). Signalling mechanisms mediating neuronal responses to guidance cues. *Nat. Rev. Neurosci.* **4**, 941-956.

Hakeda-Suzuki, S., Ng, J., Tzu, J., Dietzl, G., Sun, Y., Harms, M., Nardine, T., Luo, L. and Dickson, B. J. (2002). Rac function and regulation during Drosophila development. *Nature* **416**, 438-442.

Harris, R., Sabatelli, L. M. and Seeger, M. A. (1996). Guidance cues at the Drosophila CNS midline: identification and characterization of two Drosophila Netrin/UNC-6 homologs. *Neuron* **17**, 217-228.

Hsouna, A., Kim, Y. S. and VanBerkum, M. F. (2003). Abelson tyrosine kinase is required to transduce midline repulsive cues. *J. Neurobiol.* **57**, 15-30.

Huber, A. B., Kolodkin, A. L., Ginty, D. D. and Cloutier, J. F. (2003). Signaling at the growth cone: ligand-receptor complexes and the control of axon growth and guidance. *Annu. Rev. Neurosci.* **26**, 509-563.

Hummel, T., Schimmelpfeng, K. and Klambt, C. (1999a). Commissure

formation in the embryonic CNS of Drosophila. I. Identification of the required gene functions. *Development* **126**, 771-779.

Hummel, T., Schimmelpfeng, K. and Klambt, C. (1999b). Commissure formation in the embryonic CNS of Drosophila. II. Function of the different midline cells. *Dev. Biol.* **209**, 381-398.

Keino-Masu, K., Masu, M., Hinck, L., Leonardo, E. D., Chan, S. S., Culotti, J. G. and Tessier-Lavigne, M. (1996). Deleted in Colorectal Cancer (DCC) encodes a netrin receptor. *Cell* **87**, 175-185.

Kidd, T., Brose, K., Mitchell, K. J., Fetter, R. D., Tessier-Lavigne, M., Goodman, C. S. and Tear, G. (1998). Roundabout controls axon crossing of the CNS midline and defines a novel subfamily of evolutionarily conserved guidance receptors. *Cell* **92**, 205-215.

Kidd, T., Bland, K. S. and Goodman, C. S. (1999). Slit is the midline repellent for the robo receptor in Drosophila. *Cell* **96**, 785-794.

Kim, Y. S., Fritz, J. L., Seneviratne, A. K. and VanBerkum, M. F. (2002). Constitutively active myosin light chain kinase alters axon guidance decisions in Drosophila embryos. *Dev. Biol.* **249**, 367-381.

Kolodziej, P. A., Timpe, L. C., Mitchell, K. J., Fried, S. R., Goodman, C. S., Jan, L. Y. and Jan, Y. N. (1996). frazzled encodes a Drosophila member of the DCC immunoglobulin subfamily and is required for CNS and motor axon guidance. *Cell* **87**, 197-204.

Krause, M., Dent, E. W., Bear, J. E., Loureiro, J. J. and Gertler, F. B. (2003). Ena/VASP proteins: regulators of the actin cytoskeleton and cell migration. *Annu. Rev. Cell Dev. Biol.* **19**, 541-564.

Kwiatkowski, A. V., Gertler, F. B. and Loureiro, J. J. (2003). Function and regulation of Ena/VASP proteins. *Trends Cell Biol.* **13**, 386-392.

Lanier, L. M. and Gertler, F. B. (2000). From Abl to actin: Abl tyrosine kinase and associated proteins in growth cone motility. *Curr. Opin. Neurobiol.* **10**, 80-87.

Lebrand, C., Dent, E. W., Strasser, G. A., Lanier, L. M., Krause, M., Svitkina, T. M., Borisy, G. G. and Gertler, F. B. (2004). Critical role of Ena/VASP proteins for filopodia formation in neurons and in function downstream of netrin-1. *Neuron* **42**, 37-49.

Lee, H. and Van Vactor, D. (2003). Neurons take shape. *Curr. Biol.* **13**, R152-R161.

Li, W., Lee, J., Vikis, H. G., Lee, S. H., Liu, G., Aurandt, J., Shen, T. L., Fearon, E. R., Guan, J. L., Han, M. et al. (2004). Activation of FAK and Src are receptor-proximal events required for netrin signaling. *Nat. Neurosci.* **7**, 1213-1221.

Li, X., Meriane, M., Triki, I., Shekarabi, M., Kennedy, T. E., Larose, L. and Lamarche-Vane, N. (2002a). The adaptor protein Nck-1 couples the netrin-1 receptor DCC (deleted in colorectal cancer) to the activation of the small GTPase Rac1 through an atypical mechanism. *J. Biol. Chem.* **277**, 37788-37797.

Li, X., Saint-Cyr-Proulx, E., Aktories, K. and Lamarche-Vane, N. (2002b). Rac1 and Cdc42 but not RhoA or Rho kinase activities are required for neurite outgrowth induced by the Netrin-1 receptor DCC (deleted in colorectal cancer) in N1E-115 neuroblastoma cells. *J. Biol. Chem.* **277**, 15207-15314.

Liebl, E. C., Forsthoefel, D. J., Franco, L. S., Sample, S. H., Hess, J. E., Cowger, J. A., Chandler, M. P., Shupert, A. M. and Seeger, M. A. (2000). Dosage-sensitive, reciprocal genetic interactions between the Abl tyrosine kinase and the putative GEF trio reveal trio's role in axon pathfinding. *Neuron* **26**, 107-118.

Liebl, E. C., Rowe, R. G., Forsthoefel, D. J., Stammler, A. L., Schmidt, E. R., Turski, M. and Seeger, M. A. (2003). Interactions between the secreted protein Amalgam, its transmembrane receptor Neurotactin and the Abelson tyrosine kinase affect axon pathfinding. *Development* **130**, 3217-3226.

Liu, G., Beggs, H., Jurgensen, C., Park, H. T., Tang, H., Gorski, J., Jones, K. R., Reichardt, L. F., Wu, J. and Rao, Y. (2004). Netrin requires focal adhesion kinase and Src family kinases for axon outgrowth and attraction. *Nat. Neurosci.* **7**, 1222-1232.

Luo, L. (2000). Rho GTPases in neuronal morphogenesis. *Nat. Rev. Neurosci.* **1**, 173-180.

Luo, L. (2002). Actin cytoskeleton regulation in neuronal morphogenesis and structural plasticity. *Annu. Rev. Cell Dev. Biol.* **18**, 601-635.

Matsuura, R., Tanaka, H. and Go, M. J. (2004). Distinct functions of Rac1 and Cdc42 during axon guidance and growth cone morphogenesis in Drosophila. *Eur. J. Neurosci.* **19**, 21-31.

Meriane, M., Tcherkezian, J., Webber, C. A., Danek, E. I., Triki, I., McFarlane, S., Bloch-Gallego, E. and Lamarche-Vane, N. (2004). Phosphorylation of DCC by Fyn mediates Netrin-1 signaling in growth cone guidance. *J. Cell Biol.* **167**, 687-698.

Mitchell, K. J., Doyle, J. L., Serafini, T., Kennedy, T. E., Tessier-Lavigne, M., Goodman, C. S. and Dickson, B. J. (1996). Genetic analysis of Netrin genes in Drosophila: Netrins guide CNS commissural axons and peripheral motor axons. *Neuron* **17**, 203-215.

Moresco, E. M. and Koleske, A. J. (2003). Regulation of neuronal morphogenesis and synaptic function by Abl family kinases. *Curr. Opin. Neurobiol.* **13**, 535-544.

Muda, M., Worby, C. A., Simonson-Leff, N., Clemens, J. C. and Dixon, J. E. (2002). Use of double-stranded RNA-mediated interference to determine the substrates of protein tyrosine kinases and phosphatases. *Biochem. J.* **366**, 73-77.

Onel, S., Bolke, L. and Klambt, C. (2004). The *Drosophila* ARF6-GEF Schizo controls commissure formation by regulating Slit. *Development* **131**, 2587-2594.

Patel, B. N. and Van Vactor, D. L. (2002). Axon guidance: the cytoplasmic tail. *Curr. Opin. Cell Biol.* **14**, 221-229.

Patel, N. H., Snow, P. M. and Goodman, C. S. (1987). Characterization and cloning of fasciclin III: a glycoprotein expressed on a subset of neurons and axon pathways in Drosophila. *Cell* **48**, 975-988.

Rajagopalan, S., Vivancos, V., Nicolas, E. and Dickson, B. J. (2000). Selecting a longitudinal pathway: Robo receptors specify the lateral position of axons in the Drosophila CNS. *Cell* **103**, 1033-1045.

Ratnaparkhi, A., Banerjee, S. and Hasan, G. (2002). Altered levels of Gq activity modulate axonal pathfinding in Drosophila. *J. Neurosci.* **22**, 4499-4508.

Ren, X. R., Ming, G. L., Xie, Y., Hong, Y., Sun, D. M., Zhao, Z. Q., Feng, Z., Wang, Q., Shim, S., Chen, Z. F. et al. (2004). Focal adhesion kinase in netrin-1 signaling. *Nat. Neurosci.* **7**, 1204-1212.

Rothberg, J. M., Hartley, D. A., Walther, Z. and Artavanis-Tsakonas, S. (1988). slit: an EGF-homologous locus of D. melanogaster involved in the development of the embryonic central nervous system. *Cell* **55**, 1047-1059.

Seeger, M., Tear, G., Ferres-Marco, D. and Goodman, C. S. (1993). Mutations affecting growth cone guidance in Drosophila: genes necessary for guidance toward or away from the midline. *Neuron* **10**, 409-426.

Shekarabi, M. and Kennedy, T. E. (2002). The netrin-1 receptor DCC promotes filopodia formation and cell spreading by activating Cdc42 and Rac1. *Mol. Cell. Neurosci.* **19**, 1-17.

Simpson, J. H., Bland, K. S., Fetter, R. D. and Goodman, C. S. (2000a). Short-range and long-range guidance by Slit and its Robo receptors: a combinatorial code of Robo receptors controls lateral position. *Cell* **103**, 1019-1032.

Simpson, J. H., Kidd, T., Bland, K. S. and Goodman, C. S. (2000b). Short-range and long-range guidance by slit and its Robo receptors. Robo and Robo2 play distinct roles in midline guidance. *Neuron* **28**, 753-766.

Sini, P., Cannas, A., Koleske, A. J., Di Fiore, P. P. and Scita, G. (2004). Abl-dependent tyrosine phosphorylation of Sos-1 mediates growth-factor-induced Rac activation. *Nat. Cell. Biol.* **6**, 268-274.

Struckhoff, E. C. and Lundquist, E. A. (2003). The actin-binding protein UNC-115 is an effector of Rac signaling during axon pathfinding in C. elegans. *Development* **130**, 693-704.

Tong, J., Killeen, M., Steven, R., Binns, K. L., Culotti, J. and Pawson, T. (2001). Netrin stimulates tyrosine phosphorylation of the UNC-5 family of netrin receptors and induces Shp2 binding to the RCM cytodomain. *J. Biol. Chem.* **276**, 40917-40925.

Turner, M. and Billadeau, D. D. (2002). VAV proteins as signal integrators for multi-subunit immune-recognition receptors. *Nat. Rev. Immunol.* **2**, 476-486.

Van Etten, R. A. (1999). Cycling, stressed-out and nervous: cellular functions of c-Abl. *Trends Cell Biol.* **9**, 179-186.

Wadsworth, S. C., Madhavan, K. and Bilodeau-Wentworth, D. (1985). Maternal inheritance of transcripts from three Drosophila src-related genes. *Nucl. Acids Res.* **13**, 2153-2170.

Wills, Z., Bateman, J., Korey, C. A., Comer, A. and Van Vactor, D. (1999). The tyrosine kinase Abl and its substrate enabled collaborate with the receptor phosphatase Dlar to control motor axon guidance. *Neuron* **22**, 301-312.

Wills, Z., Emerson, M., Rusch, J., Bikoff, J., Baum, B., Perrimon, N. and Van Vactor, D. (2002). A Drosophila homolog of cyclase-associated proteins collaborates with the Abl tyrosine kinase to control midline axon pathfinding. *Neuron* **36**, 611-622.

Woodring, P. J., Hunter, T. and Wang, J. Y. (2003). Regulation of F-actin-dependent processes by the Abl family of tyrosine kinases. *J. Cell Sci.* **116**, 2613-2626.

Yu, T. W., Hao, J. C., Lim, W., Tessier-Lavigne, M. and Bargmann, C. I. (2002). Shared receptors in axon guidance: SAX-3/Robo signals via UNC-34/Enabled and a Netrin-independent UNC-40/DCC function. *Nat. Neurosci.* **5**, 1147-1154.

Table S1. Organization of longitudinally projecting axons is affected by mutations in *Abl*, *trio*, *fra*, *ena* and the *Netrin* genes

Genotype	% Hemisegments with fascicle breaks* (*n*=total hemisegments scored)			% Hemisegments with fascicle fusions† (*n*=total hemisegments scored)		
	Mild (1-2)	Severe/complete (3)	Total (*n*)	Mild (1-2)	Severe/all (3)	Total (*n*)
Wild type	0.9	0	0.9 (220)	1.4	0	1.4 (220)
fra^4/fra^4	19.3	0	19.3 (176)	12.5	5.1	17.6 (176)
$fra^4/Df(2R)vg135$	5.6	0	5.6 (198)	6.1	1.5	7.6 (198)
Df(1)NP5/Y	12.7	0.4	13.2 (228)	15.4	4.4	19.7 (228)
Abl^4/Abl^1	15.7	0	15.7 (198)	6.6	1.5	8.1 (198)
$fra^4/+;Abl^4/Abl^1$	8.6	0	8.6 (256)	2.3	0.4	2.7 (256)
$Df(3L)FpaI/trio^{IMP159.4}$	69.7	0	69.7 (208)	14.4	4.3	18.8 (208)
$fra^4/+;Df(3L)FpaI/trio^{IMP159.4}$	58.8	0.6	59.4 (170)	14.7	7.6	22.4 (170)
$fra^4/fra^4;Abl^4/+$	28.1	0.5	28.6 (196)	8.2	3.1	11.2 (196)
$fra^4/fra^4;Df(3L)FpaI/+$	28.6	0	28.6 (220)	16.4	8.6	25.0 (220)
$fra^4/fra^4;Abl^4/Abl^1$	63.1	3.1	66.3 (160)	32.5	48.8	81.3 (160)
$fra^4/fra^4;Df(3L)FpaI/trio^{M89}$	34.0	0	34.0 (212)	9.9	17.0	26.9 (212)
$Df(3L)FpaI,Abl^4/trio^{IMP159.4},Abl^1$	42.5	13.0	55.5 (200)	32.5	44.5	77.0 (200)
$fra^4,ena^{GC10}/Df(2R)vg135$	13.7	0	13.7 (124)	12.1	3.2	15.3 (124)
$Df(1)NP5/Y;ena^{23}$	3.2	0	3.2 (126)	5.6	2.4	7.9 (126)
$ena^{GC10}/+;$ $trio^{IMP159.4},Abl^1/Df(3L)FpaI,Abl^4$	22.0	1.8	23.9 (218)	11.0	67.9	78.9 (218)

Stage 17 embryos were stained with mAb 1D4 and dissected.

*Fascicle breaks were scored if one or more longitudinally projecting fascicles within the longitudinal connective were discontinuous between hemisegments.

†Fascicle 'fusions' were scored when two or three fascicles appeared to fasciculate with each other within a segment or the longitudinal connective posterior to a segment. In more severe cases, distinct fascicles could not even be distinguished, although the width of the resulting bundle or intensity of staining suggested that most axons were present, but simply had collapsed into one larger longitudinal bundle (see Fig. S1 in the supplementary material).